

Domain Wall Formation in $\text{Ni}_x\text{Fe}_{1-x}$

P. Weinberger

Center for Computational Materials Science, Technical University of Vienna, Getreidemarkt 9/134, A-1060 Vienna, Austria
(Received 25 September 2006; published 12 January 2007)

In terms of a multiscale approach based on the Landau-Ginzburg expansion and on *ab initio* parameters evaluated by means of the fully relativistic screened Korringa-Kohn-Rostoker method, the width of domain walls is evaluated for the whole range of concentration in $\text{Ni}_x\text{Fe}_{1-x}$. It is found that domain-wall formation occurs only for $x < 20\%$ and $x > 55\%$; i.e., in the neighborhood of the structural phase transition from bcc to fcc, $\text{Ni}_x\text{Fe}_{1-x}$ first tends to form single domains before the actual range of concentrations of this phase transition is reached. The calculated domain-wall widths are found to be in reasonably good agreement with available experimental data.

DOI: 10.1103/PhysRevLett.98.027205

PACS numbers: 75.60.Ch, 75.30.Et, 75.30.Gw

Since their discovery by Bloch [1] and Néel [2], magnetic domains and domain walls have become important features of ferromagnetism, which over more than five decades has constantly aroused curiosity; see, for example, Refs. [3–5]. Although nowadays the interest in magnetic domains and domain-wall formation has changed from extended systems such as well characterized thick layers on suitable substrates or single crystals to restricted systems in the form of thin wires or spin valve type arrangements, i.e., to systems with structural or geometrical restrictions, one has to realize that—as can be deduced from Refs. [6–8]—dynamical effects and the use of currents to induce domain-wall motions are not such new phenomena or recently discovered techniques as sometimes believed. Clearly enough, the discovery of the giant magnetoresistance effect increased substantially the interest in domain walls because of their contribution to the overall resistance of devices based on this effect. Since domain-wall widths are typically only between 100 and 500 nm, experimental techniques had to be improved continuously in order to map out sufficiently well domain walls, and, by making use of spin-polarized techniques, in the past few years have seemed to head even for a resolution necessary to trace the orientation of the magnetization within domain walls. Theoretical investigations in this context were either based on macroscopic models (see Refs. [9–12]), micromagnetic simulations [13,14], or Monte Carlo simulations [15] or were devoted to domain-wall related electric properties (see Refs. [16–18]).

Suppose a substitutional alloy is viewed as an infinite stack of atomic planes with the z axis serving as the surface normal and two-dimensional translational invariance within the planes [19]. The orientation of the magnetization in the individual planes of a system consisting of two domains and a domain wall in between can then be characterized by a set of unit vectors n_i , $|\vec{n}_i| = 1$, $\forall i$. C_i then denotes a particular magnetic configuration in the magnetic domain wall, $C_i = \{\vec{n}_l, \dots, \vec{n}_l, \vec{n}_0, \vec{n}_1, \dots, \vec{n}_L, \vec{n}_r, \dots, \vec{n}_r\}$, where \vec{n}_l and \vec{n}_r refer to the orientations in the

left and right domains, respectively, and L is the width of the domain wall in monolayers (ML). By making use of the so-called magnetic force theorem, the energy difference between this configuration and a given reference configuration C_0 , e.g., $C_0 = \{\vec{n}_i = \vec{n}_l, \forall i\}$, can then be expressed as the difference in grand potentials:

$$\Delta E(C_i, L) = E(C_i, L) - E(C_0, L), \quad (1)$$

$$E(C_i, L) = \int_{E_b}^{E_F} n(C_i, L; \epsilon) (\epsilon - E_F) d\epsilon, \quad (2)$$

where $n(C_i, L; \epsilon)$ is the density of states (in L unit cells) corresponding to the configuration C_i , and E_b and E_F denote the valence band bottom and the Fermi energy, respectively. In principle, in order to obtain at a given width L the domain-wall formation energy, the minimum over all configurations C_i has to be evaluated, $E(L) = \min_{\{C_i\}} [\Delta E(C_i, L)]$. Here, however, this general description is restricted to $E(L) = E(C_1, L) - E(C_0, L)$, $C_1: \vec{n}_l = \vec{x}$, $\vec{n}_r = -\vec{x}$, $\vec{n}_i = D(\Phi_i)\vec{x}$, $\Phi_i = 180i/L$, $i = 1, \dots, L$, with \vec{x} being a unit vector in the planes of atoms and $D(\Phi_i)$ a rotation by an angle Φ_i around the surface normal [19].

It was discussed in quite some detail in Ref. [20] that a phenomenological description [21] of the grand potential $E(L)$ can be applied in a kind of multiscale approach in order to predict the equilibrium domain-wall width L_0 by making use of *ab initio* parameters. In this simplified description, $E(L)$ is defined as

$$E(L) = E(C_1, L) - E(C_0, L) = A_0 \left(\frac{\alpha}{L} + \beta L \right), \quad (3)$$

where A_0 is the area of the two-dimensional unit cell, and α and β are proportional to the exchange and magnetic anisotropy energy, respectively. From the condition $dE(L)/dL = 0$ follows immediately that the equilibrium domain-wall width L_0 is given by $L_0 = \sqrt{\alpha/\beta}$. The coefficients α and β in Eq. (3) can easily be obtained by evaluating $E(L)$ by means of an *ab initio* method at two different values of L , say, L_1 and L_2 , $L_2 > L_1$, since

$$\beta = [L_2 E(L_2) - L_1 E(L_1)] / (L_2^2 - L_1^2),$$

$$\alpha = L_1 E(L_1) - \beta L_1^2. \quad (4)$$

Furthermore, for $L_2 - L_1 = n$ the corresponding energy difference $\Delta E(n) = E(L_1 + n) - E(L_1)$ is simply given by $\Delta E(n) = -\alpha n / (L_1^2 + L_1 n) + n\beta \approx n\beta$.

All *ab initio* calculations were performed using the spin-polarized relativistic screened Korringa-Kohn-Rostoker method in the atomic sphere approximation (for details, see Ref. [22]) and the local density functional parametrization given in Ref. [23]. For each concentration of $\text{Ni}_x\text{Fe}_{1-x}$, the effective potentials and exchange fields were calculated self-consistently at the experimental lattice spacing a by means of the inhomogeneous coherent potential approximation [22] using 45 k points in an irreducible part of the surface Brillouin zone with the orientation of the magnetization pointing uniformly along \vec{x} . Using these potentials and exchange fields, the grand potentials $E(C_i, L)$ in Eq. (2) were evaluated by means of a contour

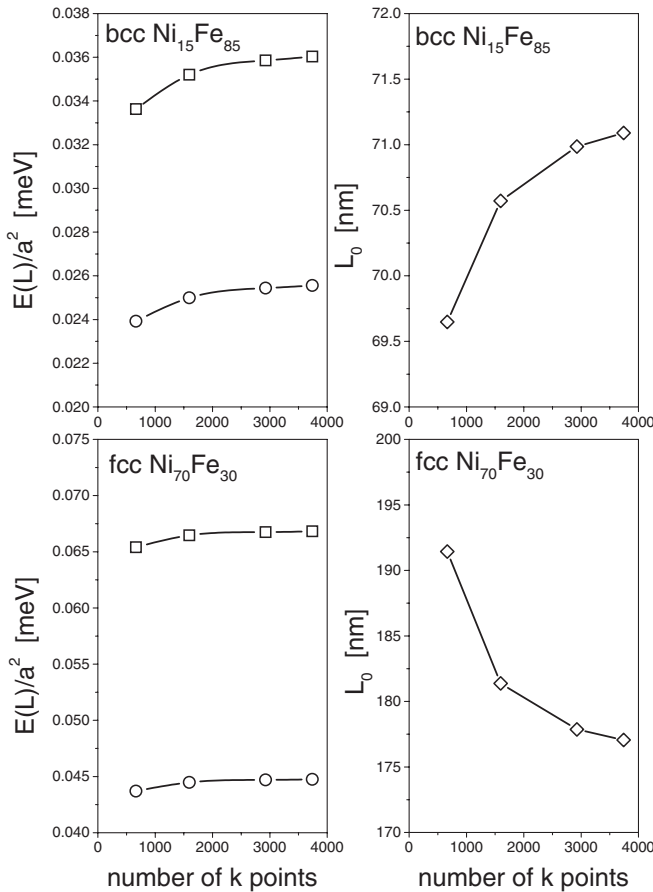


FIG. 1. Convergence of the domain-wall formation energy $E(L)/a^2$ (left, squares: $L = 126$ ML, circles: $L = 192$ ML) and of the equilibrium domain-wall width L_0 in nanometers (right) with respect to the number of k points used in the surface Brillouin zone integrations. a refers to the lattice constant.

integration along a semicircle using a 16 point Gaussian quadrature.

In the left part of Fig. 1, the convergence of $E(L)$ with respect to the number of k points used in the surface Brillouin zone integrations is shown for domain-wall widths of $L_1 = 126$ and $L_2 = 192$ ML for bcc $\text{Ni}_{15}\text{Fe}_{85}$ and fcc $\text{Ni}_{70}\text{Fe}_{30}$. In the right part of this figure, the corresponding convergence of L_0 is displaced using this choice of L_1 and L_2 in Eq. (4). It turns out that by increasing the number of k points beyond 3000 in these two cases the remaining error for the equilibrium domain-wall width L_0 is less than 1%.

In Fig. 2, the domain-wall formation energies $E(L)/a^2$ are displayed versus L (in nanometers) for bcc $\text{Ni}_{15}\text{Fe}_{85}$ and fcc $\text{Ni}_{85}\text{Fe}_{15}$. In this figure, the corresponding solid line refers to a fit using $L_1 = 126$ ML and $L_2 = 192$ ML,

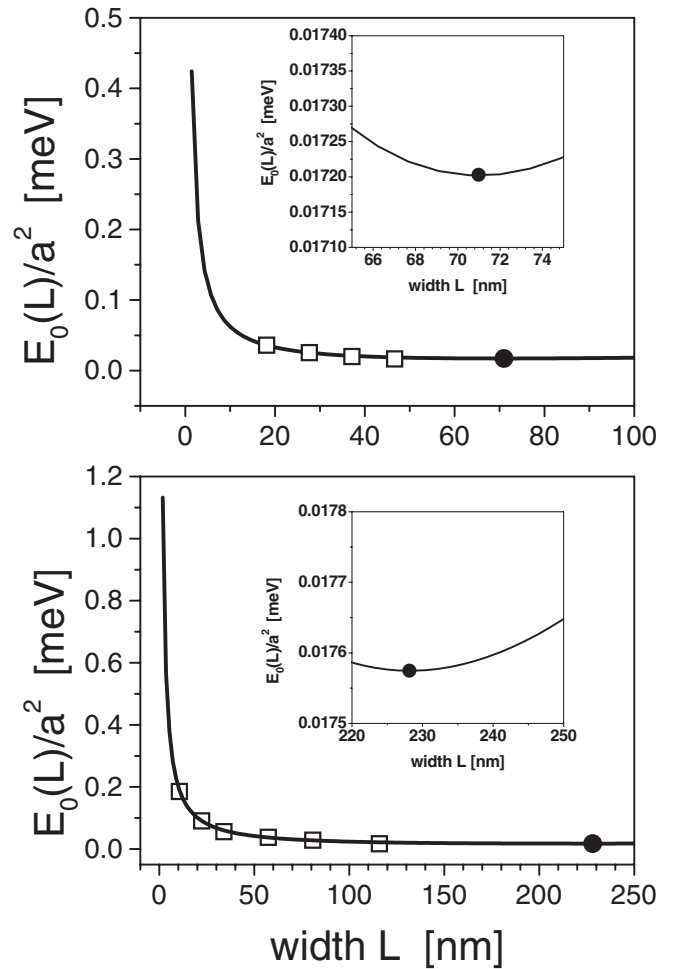


FIG. 2. Domain-wall formation energies $E(L)/a^2$ for bcc $\text{Ni}_{15}\text{Fe}_{85}$ and fcc $\text{Ni}_{85}\text{Fe}_{15}$ as a function of the domain-wall width L . Open squares refer to calculated values using 2926 k points in the surface Brillouin zone. The solid line corresponds to a Landau-Ginzburg fit using $L_1 = 126$ and $L_2 = 192$ ML. The position of the equilibrium domain-wall width L_0 is indicated as a solid circle. The inset shows $E(L)/a^2$ in the vicinity of L_0 .

while open squares refer to *ab initio* calculated values. Since the functional form in Eq. (3) fits very well the *ab initio* data, the occurring deviations being minute, Eq. (3) indeed can be used to predict L_0 indicated in this figure as a solid circle; see also the respective insets, in which $E(L)/a^2$ is depicted in the vicinity of L_0 .

In plotting now the value of L_0 versus the Ni concentration (see Fig. 3), a perhaps surprising feature becomes apparent: Domain walls are formed only in the bcc regime for $x < 20\%$ and in the fcc regime for $x > 55\%$, since in the remainder of concentrations $\alpha/\beta < 0$. Recalling that the structural phase transition between bcc and fcc occurs around 35% Ni, the present calculations show that, with increasing Ni concentration slightly before (bcc) or after (fcc) the concentration range of this transition is reached, $\text{Ni}_x\text{Fe}_{1-x}$ alloys tend to form single domains. Whether or not this peculiar feature is, in fact, already part of the causes driving the structural phase transition seems to belong rather to the realm for speculations and qualitative arguments, which shall not be entered into here.

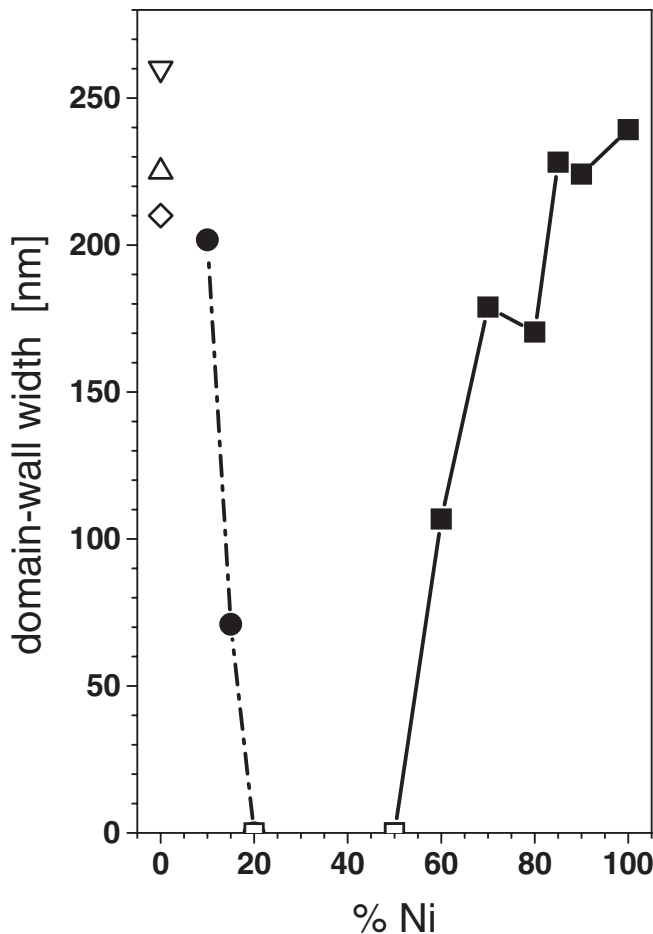


FIG. 3. Equilibrium domain-wall width L_0 (solid circles: bcc, solid squares: fcc) as a function of the Ni concentration. Note that between about 17.5% and 55% Ni no domain-wall formation occurs. The open diamond, up triangle, and down triangle refer, respectively, to Refs. [25,3,8].

Finally, in Fig. 4, the constants α and β are displayed for the fcc regime versus the Ni concentration. In particular, from this figure one can see that below 60% α and β tend to negative values.

$\text{Ni}_x\text{Fe}_{1-x}$ alloys show quite a few surprising properties. Magnetic anisotropy properties, e.g., were studied [24] over the whole concentration range for bulk and free surfaces and revealed that in the fcc regime the magnetic anisotropies were indeed very tiny. It should be noted that, just as for the present problem, for a theoretical description of these anisotropy properties a fully relativistic description is necessary.

As already stated, a direct measurement of the width of domain walls is a rather subtle task, since not only do geometric restrictions play a crucial role but also the shape of the sample (films or wires) matters. It is therefore not

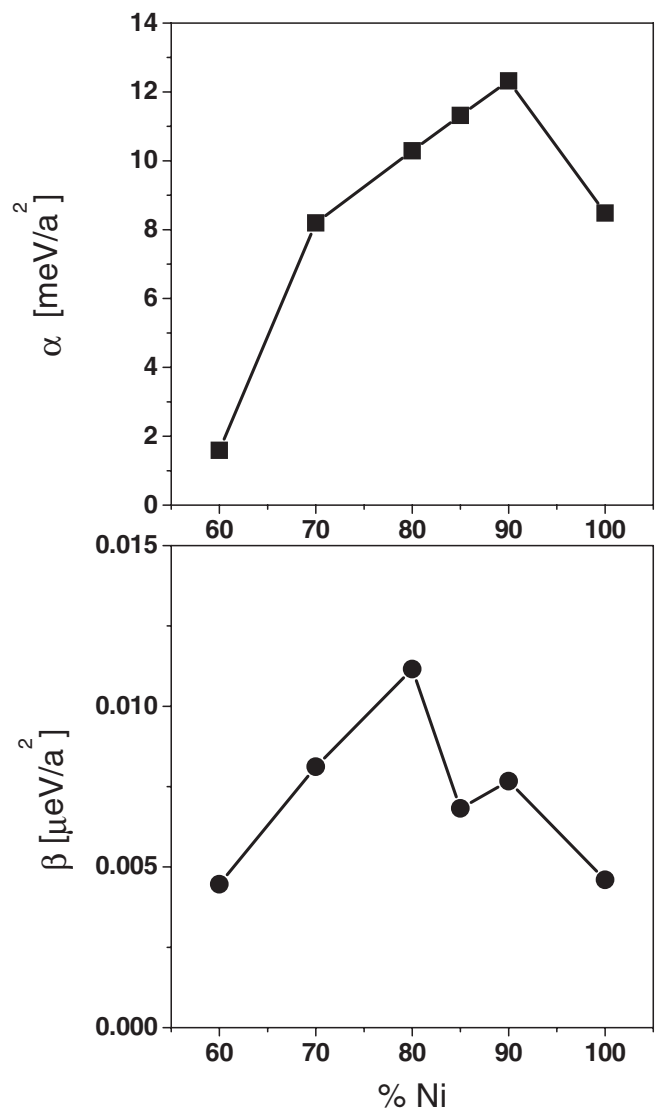


FIG. 4. Evaluated constants α and β for the fcc regime of $\text{Ni}_x\text{Fe}_{1-x}$. All calculations are based on the use of 2926 k points in the surface Brillouin zone; see also Fig. 1.

surprising at all that only in the case where comparable shapes were considered are somewhat similar experimental data to be found in the literature. For Fe(100) single crystals, a width W of 135 ± 25 nm is reported [25], whereby the authors of this reference explicitly note that their 180° domain walls were “by no means of Bloch type.” They also argue that the domain-wall width is the same in the bulk and at the surface. In using the relation $W = (2/\pi)W_L$, where W_L is the width of the rotation angle of the magnetization [3], W_L turns out to be 210 ± 40 nm, which is in reasonably good agreement with the data reported earlier by Hartmann and Mende [6] (228 nm), Lilley [3] (225 nm), and Suzuki and Suzuki [8] (260 nm).

Depending on the film thickness, by the use of high resolution Lorentz microscopy a direct observation of a domain wall yielded a width between 60 and 210 nm for $\text{Ni}_{81}\text{Fe}_{19}$ [26]. Spin currents were reported [27] to create vortex walls in $\text{Ni}_{80}\text{Fe}_{20}$ with a width of 400–600 nm. However, geometrical restrictions in $\text{Ni}_{80}\text{Fe}_{20}$ seemed to result in widths between 500 and 700 nm [28]. Furthermore, for $\text{Ni}_{76}\text{Fe}_{24}$, widths between 200 and 400 nm depending on the film size were observed [7]. The calculated values in Fig. 3 of 200–250 nm for Ni concentrations larger than about 80% seem therefore to be quite reasonable in comparison to these experimental findings. Very clear statements of whether Bloch or Néel domain walls were seen experimentally are missing completely.

Quite clearly, nowadays the emphasis has shifted to domain-wall depinning by spin currents [29,30] and to domain-wall motions in the context of tunnel junctionlike trilayers [31]. However, the question of the width of domain walls in one of the most prominent magnetic systems, namely, $\text{Ni}_x\text{Fe}_{1-x}$, and of how to describe this width theoretically remains valid also in these new areas of interest. If the problem to be investigated condenses to the question of how to reduce the domain-wall width in permalloy, then Fig. 3 gives a straightforward answer.

The author thanks Professor B. L. Gyorffy for innumerable discussions over the years. Domain walls were only one of the topics touched.

-
- [1] F. Bloch, Z. Phys. **74**, 295 (1932).
 - [2] L. Néel, Cahiers de Physique **25**, 1 (1944).
 - [3] B. A. Lilley, Philos. Mag. **41**, 792 (1950).
 - [4] R. W. DeBlois, J. Appl. Phys. **29**, 459 (1958).
 - [5] L. Berger, J. Appl. Phys. **49**, 2156 (1978).
 - [6] U. Hartmann and H. H. Mende, J. Appl. Phys. **59**, 4123 (1986); Phys. Rev. B **33**, 4777 (1986).

- [7] T. Suzuki, C. H. Wilts, and C. E. Patton, J. Appl. Phys. **39**, 1983 (1968).
- [8] T. Suzuki and K. Suzuki, IEEE Trans. Magn. **13**, 1505 (1977).
- [9] A. Aharoni and J. P. Jakubovics, Phys. Rev. B **43**, 1290 (1991).
- [10] S. Müller-Pfeiffer, M. Schneider, and W. Zinn, Phys. Rev. B **49**, 15 745 (1994).
- [11] H.-B. Braun, J. Kyriakidis, and D. Loss, Phys. Rev. B **56**, 8129 (1997).
- [12] R. Hertel and H. Kronmüller, Phys. Rev. B **60**, 7366 (1999).
- [13] M. Redjfal, T. Trunk, M. F. Ruane, and F. B. Humphrey, IEEE Trans. Magn. **36**, 3071 (2000).
- [14] W. Scholz, D. Suess, T. Schrefl, and J. Fidler, J. Appl. Phys. **91**, 7047 (2002).
- [15] E. Y. Vedmedenko, A. Kubetzka, K. von Bergmann, O. Pietsch, M. Bode, J. Kirschner, H. P. Oepen, and R. Wiesendanger, Phys. Rev. Lett. **92**, 077207 (2004).
- [16] P. M. Levy and S. Zhang, Phys. Rev. Lett. **79**, 5110 (1997).
- [17] S. Gallego, P. Weinberger, L. Szunyogh, P. M. Levy, and C. Sommers, Phys. Rev. B **68**, 054406 (2003).
- [18] J. Velev and W. H. Butler, Phys. Rev. B **69**, 094425 (2004).
- [19] P. Weinberger, Philos. Mag. B **75**, 509 (1997).
- [20] J. Schwitalla, B. L. Gyorffy, and L. Szunyogh, Phys. Rev. B **63**, 104423 (2001).
- [21] See, e.g., A. M. Kosevich, in *Modern Problems in Condensed Matter Sciences*, edited by V. M. Agranovich and A. A. Maradudin (North-Holland, Amsterdam, 1986), Vol. 17, p. 495.
- [22] J. Zablouil, R. Hammerling, L. Szunyogh, and P. Weinberger, *Electron Scattering in Solid Matter* (Springer, Berlin, 2004).
- [23] S. H. Vosko, L. Wilk, and M. Nusair, Can. J. Phys. **58**, 1200 (1980).
- [24] P. Weinberger, L. Szunyogh, B. Blaas, C. Sommers, and P. Entel, Phys. Rev. B **63**, 094417 (2001).
- [25] H. P. Oepen and J. Kirschner, Phys. Rev. Lett. **62**, 819 (1989).
- [26] B. Y. Wong and D. E. Laughlin, J. Appl. Phys. **79**, 6455 (1996).
- [27] M. Kläui, P.-O. Jubert, R. Allenspach, A. Bischof, J. A. C. Bland, G. Faini, U. Rüdiger, C. A. F. Vaz, L. Vila, and C. Vouille, Phys. Rev. Lett. **95**, 026601 (2005).
- [28] P.-O. Jubert, R. Allenspach, and A. Bischof, Phys. Rev. B **69**, 220410(R) (2004).
- [29] T. Kimura, Y. Otani, I. Yagi, K. Tsukagoshi, and Y. Aoyagi, J. Appl. Phys. **94**, 7266 (2003).
- [30] T. Kimura, Y. Otani, K. Tsukagoshi, and Y. Aoyagi, J. Appl. Phys. **94**, 7947 (2003).
- [31] K. Fukumoto, W. Kuch, J. Vogel, F. Romanens, S. Pizzini, J. Camarero, M. Binfim, and J. Kirschner, Phys. Rev. Lett. **96**, 097204 (2006).